

Provided for non-commercial research and education use.  
Not for reproduction, distribution or commercial use.



This article appeared in a journal published by Elsevier. The attached copy is furnished to the author for internal non-commercial research and education use, including for instruction at the authors institution and sharing with colleagues.

Other uses, including reproduction and distribution, or selling or licensing copies, or posting to personal, institutional or third party websites are prohibited.

In most cases authors are permitted to post their version of the article (e.g. in Word or Tex form) to their personal website or institutional repository. Authors requiring further information regarding Elsevier's archiving and manuscript policies are encouraged to visit:

<http://www.elsevier.com/copyright>



Contents lists available at ScienceDirect

Biochimica et Biophysica Acta

journal homepage: [www.elsevier.com/locate/bbabio](http://www.elsevier.com/locate/bbabio)

## The cytochrome *ba* complex from the thermoacidophilic crenarchaeote *Acidianus ambivalens* is an analog of *bc*<sub>1</sub> complexes

Tiago M. Bandejas<sup>a</sup>, Patricia N. Refojo<sup>a</sup>, Smilja Todorovic<sup>a</sup>, Daniel H. Murgida<sup>b,1</sup>, Peter Hildebrandt<sup>b</sup>, Christian Bauer<sup>c</sup>, Manuela M. Pereira<sup>a,\*</sup>, Arnulf Kletzin<sup>c</sup>, Miguel Teixeira<sup>a,\*</sup>

<sup>a</sup> Instituto de Tecnologia Química e Biológica, Universidade Nova de Lisboa, Av. da República -EAN, 2780-157 Oeiras, Portugal

<sup>b</sup> Max-Volmer-Laboratorium für Biophysikalische Chemie, Institut für Chemie, Technische Universität Berlin, Sekr. PC14, Strasse des 17. Juni 135, D-10623 Berlin, Germany

<sup>c</sup> Institute of Microbiology and Genetics, Darmstadt University of Technology, Schnittspahnstrasse 10, 64287 Darmstadt, Germany

### ARTICLE INFO

#### Article history:

Received 27 June 2008

Received in revised form 17 September 2008

Accepted 18 September 2008

Available online 1 October 2008

#### Keywords:

Archaea

*bc*<sub>1</sub> complex

Rieske

Cytochrome *b*

*b*<sub>6</sub>*f* complex

Sulfolobales

### ABSTRACT

A novel cytochrome *ba* complex was isolated from aerobically grown cells of the thermoacidophilic archaeon *Acidianus ambivalens*. The complex was purified with two subunits, which are encoded by the *cbsA* and *soxN* genes. These genes are part of the pentacistronic *cbsAB–soxLN–odsN* locus. The spectroscopic characterization revealed the presence of three low-spin hemes, two of the *b* and one of the *a*<sub>s</sub>-type with reduction potentials of +200, +400 and +160 mV, respectively. The SoxN protein is proposed to harbor the heme *b* of lower reduction potential and the heme *a*<sub>s</sub>, and CbsA the other heme *b*. The *soxL* gene encodes a Rieske protein, which was expressed in *E. coli*; its reduction potential was determined to be +320 mV. Topology predictions showed that SoxN, CbsB and CbsA should contain 12, 9 and one transmembrane  $\alpha$ -helices, respectively, with SoxN having a predicted fold very similar to those of the cytochromes *b* in *bc*<sub>1</sub> complexes. The presence of two quinol binding motifs was also predicted in SoxN. Based on these findings, we propose that the *A. ambivalens* cytochrome *ba* complex is analogous to the *bc*<sub>1</sub> complexes of bacteria and mitochondria, however with distinct subunits and heme types.

© 2008 Elsevier B.V. All rights reserved.

### 1. Introduction

The hyperthermophilic and acidophilic crenarchaeote *Acidianus* (*A. ambivalens*) grows optimally at 80 °C and pH 2.5. When grown aerobically, elemental sulfur is used as electron source and its oxidation is linked to a membrane-bound electron transfer chain that allows oxidative phosphorylation for energy conservation. One of its oxygen reductases, a quinol oxidase, has been extensively studied [1–5] and until recently it was assumed that an equivalent of the mitochondrial complex III (*bc*<sub>1</sub> complex) was absent from its respiratory chain.

Complex III catalyzes the transfer of two electrons from ubiquinol to cytochrome *c* and it is the central component of mitochondrial and of many bacterial respiratory chains. In mitochondria, the reaction is coupled to the translocation of four protons across the inner membrane via a Q-cycle mechanism [6]. The mitochondrial *bc*<sub>1</sub> complex has 11 subunits, but the minimal functional unit present in some prokaryotes contains only three subunits (e.g. *Paracoccus*

*denitrificans* [7], *Rhodobacter capsulatus* [8] and *Rhodospirillum rubrum* [9]). This minimal functional unit includes: a cytochrome *b* harboring two low-spin hemes located in opposite sides of the membrane, one of them with a low reduction potential (cyt *b*<sub>L</sub>) and the other with a high reduction potential (cyt *b*<sub>H</sub>); a high reduction potential Rieske iron–sulfur protein, and a cytochrome *c*<sub>1</sub>.

A canonical *bc*<sub>1</sub> complex has not yet been isolated from any archaeon; however, analysis of the genomes revealed that homologues of the cytochrome *b* and of the Rieske proteins are present in archaea like *Sulfolobus acidocaldarius* [10], *Aeropyrum pernix* [11] and *Thermoplasma acidophilum* [12]. No homologue of cytochrome *c*<sub>1</sub> was identified so far. The major evidence for the existence of an archaeal *bc*<sub>1</sub>-analogous complex was obtained for the euryarchaeon *Halobacterium salinarum* [13]. Cytochromes *b* and *c* associated with a Rieske iron–sulfur cluster were isolated from the membranes of this organism, but their genes remained unknown. This protein complex was shown to have an ubiquinol–cytochrome *c* oxidoreductase activity sensitive to antimycin and myxothiazol, typical inhibitors of *bc*<sub>1</sub> complexes. Also, two membrane-bound Rieske proteins (SoxF and SoxL) were isolated from the crenarchaeon *S. acidocaldarius* [10]. The SoxF protein is part of the six subunits, so-called SoxM supercomplex (*soxMEFGHI*) [14], which comprises features of both a *bc*<sub>1</sub>-analogous complex and a heme–copper oxygen reductase. SoxF (Rieske subunit) together with SoxG (cytochrome *b* subunit), which has two *a*<sub>s</sub> hemes, constitute the analogous subunits of complex III in that supercomplex.

Abbreviations: DDM, n-Dodecyl  $\beta$ -D-maltoside; IPTG, isopropyl  $\beta$ -D-1-thiogalactopyranoside

\* Corresponding authors. Tel.: +351 214469 321; fax: +351 2144269314.

E-mail addresses: [mpereira@itqb.unl.pt](mailto:mpereira@itqb.unl.pt) (M.M. Pereira), [miguel@itqb.unl.pt](mailto:miguel@itqb.unl.pt) (M. Teixeira).

<sup>1</sup> Present address: Departamento de Química Inorgánica, Analítica y Química Física / INQUIMAE-CONICET, Facultad de Ciencias Exactas y Naturales, Universidad de Buenos Aires. Ciudad Universitaria, Pab. 2, piso 1, C1428EHA-Buenos Aires, Argentina.

The subunits SoxM and SoxH compose the heme-copper reductase enzyme. SoxE is a sulfocyanine that may function as an electron carrier between the complex III analogue and the oxygen reductase. The SoxL protein encoded by the *soxL* gene is part of the *cbsAB–soxLN–odsN* locus found in *S. acidocaldarius* (DSM 639) [15].

This work reports the purification and the spectroscopic and biochemical characterization of an archaeal cytochrome *ba* complex formed by the SoxN and CbsA proteins present in the membranes of *A. ambivalens*. Heterologous expression of the *soxL* gene in *E. coli* was used to investigate the properties of the Rieske protein. Our data suggest that these proteins may constitute a quinol-oxidizing *bc*<sub>1</sub>-analogous complex, with prosthetic groups functionally similar to those of the canonical complexes III from Bacteria and Eukarya.

## 2. Materials and methods

### 2.1. Cell growth and protein purification

*A. ambivalens* cell growth and the membrane fraction preparation were carried out as previously described [16]. Solubilization of the membrane fraction was performed by gentle stirring with 1 g of *n*-dodecyl  $\beta$ -D-maltoside (DDM) per g of protein for 12 h at 4 °C and subsequent ultracentrifugation at 138,000  $\times$ g for 5 h at 4 °C. The following chromatographic steps were carried out at 4 °C on a Pharmacia HiLoad system using 40 mM potassium phosphate, pH 6.5, 0.1% DDM as buffer (A). The solubilized membranes applied to a Q-Sepharose fast-flow column were eluted with a gradient from 0 to 1 M NaCl in buffer A. The cytochrome *ba* complex was eluted together with a quinol:oxygen oxidoreductase at approximately 150 mM NaCl. This fraction was loaded directly to a ceramic hydroxylapatite (HTP) column and elution was accomplished by a linear gradient until 1 M potassium phosphate. The cytochrome *ba* complex was eluted at 500 mM of potassium phosphate. This fraction was then applied to a second ceramic HTP column and the *ba* complex fraction was eluted at around 700 mM potassium phosphate. The final step of purification was performed on a gel filtration Superdex S-200 column using buffer A supplemented with 150 mM NaCl.

### 2.2. Molecular biology procedures

The N-terminal amino acid sequences (see below) were used as a query in TFASTA searches against a database of approximately 5 Mbp of partial genome sequence from *A. ambivalens*. This procedure resulted in the identification of two short contigs. The first encoded SoxL and the N-terminal part of SoxN, while the second encoded the N-terminal part of CbsA. A third contig was identified to encode the C-terminal part of SoxN and OdsN using the corresponding SoxN amino acid sequence of *Sulfolobus solfataricus* as a probe. The missing DNA sequence between the three contigs was PCR amplified from genomic *A. ambivalens* DNA with four primers (738soxn\_fwd, TCACA TGTTT AGGAA TTATT TTG and 361soxn\_rev, GAAGA ACCAT GGCGG ATAAG TTG, for the gap in the *soxN* gene, and 738soxl\_rev, CACTG GGAGA AAGGA TGGGT TTC and 122cbsa\_fwd, GCTCT TTATT CATGA TAAGA ACC, for the remaining parts of the *cbsA* and the missing *cbsB* gene). The resulting PCR products were sequenced by GATC (Konstanz, Germany) and the three contigs were assembled using the Wisconsin Package (Accelrys).

The *soxL* gene was amplified from *A. ambivalens* genomic DNA without the first 250 bp encoding a twin-arginine leader peptide by using the primers SoxL-N2 (GGT TCC ATG GCG GGA CTT AGA GTT TTG CAA CC) and SoxL-C (TTC TCT CGA GAC TGC TAC TAA ATG GGT TCT C). The 710 bp PCR product was digested with NcoI and XhoI and ligated to the vector pET28a (Novagen) previously submitted to the same digestion. *E. coli* Top10F' cells (Invitrogen) were transformed with the ligation mixture and positive clones were selected. After confirming the correct insertion of the fragment by sequencing, *E. coli* BL21, CodonPlus (DE3)-RIL competent cells (Stratagene) were transformed

with the resulting plasmid. The cells were grown in 2 $\times$ YT medium to an OD of 0.6. Gene expression was induced by addition of 0.5 mM IPTG and the cells were grown overnight. Cells were harvested by centrifugation at 10,000  $\times$ g and resuspended in 20 mM Tris–HCl pH 7.4. The cells were disrupted by a single passage through a French Press at 135 MPa and the resulting protein suspension centrifuged at 150,000  $\times$ g for 60 min. The clear supernatant was applied to a 10 mL Ni-NTA column (GE healthcare), equilibrated with the same buffer. The column was washed with 3 volumes of a buffer with 60 mM imidazole and eluted with 100 mM imidazole in the same buffer. The obtained protein was diluted with 20 mM Tris–HCl pH 7.4, containing 10% of glycerol. A Reverse Transcriptase PCR, using the primers used for the *soxL* expression and with the total RNA prepared from aerobically grown *A. ambivalens* cells, was performed in order to check that *soxL* is expressed in vivo.

### 2.3. Sequence analysis tools

Searches for similar proteins in databases were performed using the BLAST, TBLASTN, and PSI-BLAST algorithms [17] with the non-redundant Genbank databases nt and nr. Multiple alignments were performed using PILEUP (Wisconsin Package) and CLUSTAL W version 1.6 installed locally [18] or MAFFT over the Web interface [19]. The search for secondary and tertiary structure elements was done using the meta-search engine PredictProtein at <http://cubic.bioc.columbia.edu/predictprotein/> using the available tools. The search for conserved domains was done using the CD-browser at NCBI. The SoxN dendrogram was calculated using PAUPSEARCH installed locally with the Wisconsin Package on a shortened 260 amino acid residues version of the alignment without end gaps or highly divergent regions (maximum likelihood algorithm with 100 bootstrap repetitions; see [Supplementary figure S4](#)). Prediction of transmembrane helices, amino acids motifs and glycosylation sites was done using the tools available via the metaserver <http://www.expasy.org>. The SoxN protein model PDB file was generated using the ESyPred3D Web Server 1.0, which indicated the bovine mitochondrial *bc*<sub>1</sub> complex as template (1QCR, chain C) [20], (<http://www.fundp.ac.be/sciences/biologie/urbm/bioinfo/esy3d/>).

### 2.4. Analytical methods

Protein concentration was determined using the modified micro-biuret method for membrane proteins [21]. Purity of the isolated cytochrome *ba* complex was determined by SDS-PAGE with a polyacrylamide gradient gel (10–15%) as in [22]. Pyridine heme spectra of the complex was performed as previously reported [23]. Heme extraction was carried out as in [24] and the resulting extracted sample was applied to a HPLC Nova Pak C18 3.9 $\times$ 150 mm column. A gradient was applied from 75% trifluoroacetic acid solution (containing 0.5% TFA) and 25% acetonitrile (0.5% TFA) to 100% acetonitrile (0.5% TFA), and the elution profile was monitored at 406 nm. The same procedure was used with hemoglobin and *A. ambivalens* *aa*<sub>3</sub> oxygen reductase to obtain heme standards. The areas of the respective HPLC peaks were integrated. N-terminal amino acid sequences were obtained by automated Edman degradation [25], using an Applied Biosystem Model 471 H sequencer, after protein subunits separation in SDS-PAGE (10–15% polyacrylamide), followed by transfer of the peptides to a polyvinylidene difluoride membrane. Metal analysis of the purified complex was performed by X-Ray fluorescence spectroscopy (TXRF-analysis) with an EXTRAIIA instrument (Atomika Instruments) at the Institute of Inorganic and Analytical Chemistry in Frankfurt/Main (Germany).

### 2.5. Spectroscopic methods

A Shimadzu spectrophotometer (UV-1603), equipped with a temperature controller, was used to obtain UV-visible spectra and

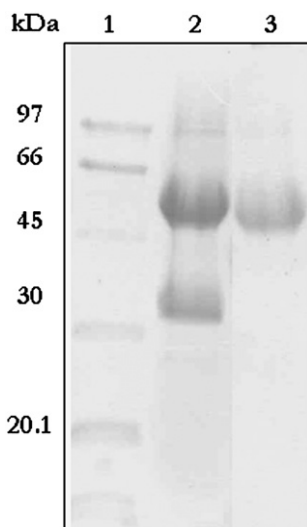


**Fig. 1.** SDS-PAGE (10–15% polyacrylamide) of the *A. ambivalens* cytochrome *ba* complex. Lane 1, molecular mass markers; lane 2, complex stained with Coomassie brilliant blue, lane 3, complex stained with Alcian blue.

monitor redox titrations. EPR spectra were recorded on a Bruker EMX spectrometer, equipped with an ESR 900 continuous-flow helium cryostat. Experimental conditions were: temperature 10 K, microwave frequency 9.39 GHz, microwave power 2.4 mW and modulation amplitude 1 mT. Resonance Raman spectra were measured in backscattering geometry using a confocal microscope coupled to a single stage spectrometer (Jobin Yvon, Oberursel, Germany) with 1800 l/mm grating and liquid nitrogen cooled CCD detector. Elastic scattering and reflected light were rejected with super notch filters. All measurements were performed at  $4\text{ cm}^{-1}$  true spectral resolution using a 413 nm excitation from a Kr ion laser (Coherent Innova 302). The sample, 100  $\mu\text{l}$  of 30  $\mu\text{M}$  protein in phosphate buffer (20 mM pH 6.5, 0.1% DDM), was placed in a rotating cuvette to minimize laser induced degradation. For the same reason, the laser power at the sample was kept below 100  $\mu\text{W}$  and accumulation times set to 10 s. Full oxidation and full reduction of the protein were achieved by addition of a small excess of  $\text{K}_2\text{IrCl}_6$  and  $\text{Na}_2\text{S}_2\text{O}_4$ , respectively, under anaerobic conditions.

2.6. Redox titrations

The anaerobic titration of *A. ambivalens* cytochrome *ba* complex ( $\sim 3.3\ \mu\text{M}$  in 40 mM potassium phosphate, pH 6.5, 0.1% DDM), monitored by UV–visible absorption spectroscopy, was performed in a cuvette continuously flushed with argon, by stepwise addition of buffered sodium dithionite. Spectra from 400 to 700 nm were obtained at each solution redox potential, after attaining equilibrium. The complete data set was analyzed using MATLAB (Mathworks, South Natick, MA, USA) for Windows. The analysis was focused at the Soret and  $\alpha$  band regions, which allowed the deconvolution of the different heme centers by inspection of the individual spectra or by means of successive subtractions. Once all optical components were identified and deconvoluted, the changes in absorbance at the corresponding maxima at the  $\alpha$  band region (561 and 574, and 585 nm for respectively hemes *b* and *a*) as a function of the solution reduction potential were used to determine the redox transitions of each heme center. The following compounds were used as redox mediators (1.5  $\mu\text{M}$  each): *N,N* dimethyl-*p*-phenylenodiamine ( $E'_o = +340\text{ mV}$ ), *p*-benzoquinone ( $E'_o = +240\text{ mV}$ ), 1,2-naphtoquinone-4-sulphonic acid ( $E'_o = +215\text{ mV}$ ), trimethylhydroquinone ( $E'_o = +115\text{ mV}$ ), phenazine methosulfate ( $E'_o = +80\text{ mV}$ ), 1,4-naphtoquinone ( $E'_o = +60\text{ mV}$ ), phenazine ethosulfate ( $E'_o = +55\text{ mV}$ ), duroquinone ( $E'_o = +5\text{ mV}$ ). Full oxidation of the complex was achieved after incubation with  $\text{K}_2\text{IrCl}_6$ . The Rieske protein in a concentration of 240  $\mu\text{M}$  in 20 mM Tris–HCl, pH 7.4, 10% glycerol was titrated using sodium dithionite and monitored by EPR spectroscopy. The following redox mediators (50  $\mu\text{M}$  each) were used: potassium ferricyanide ( $E'_o = +430\text{ mV}$ ), *N,N* dimethyl-*p*-phenylenodiamine ( $E'_o = +340\text{ mV}$ ), 1,2-naphtoquinone-4-sulphonic acid ( $E'_o = +215\text{ mV}$ ), 1,2-naphtoquinone ( $E'_o = +180\text{ mV}$ ), trimethylhydroquinone ( $E'_o = +115\text{ mV}$ ), phenazine methosulfate ( $E'_o = +80\text{ mV}$ ), 1,4-naphtoquinone ( $E'_o = +60\text{ mV}$ ), duroquinone ( $E'_o = +5\text{ mV}$ ), menadione ( $E'_o = 0\text{ mV}$ ). A combined silver/silver chloride electrode, or a silver chloride and a platinum electrode were used, calibrated against a saturated quinhydrone solution. Reduction potentials are quoted versus the standard hydrogen electrode.

3. Results and discussion

A novel two-subunit complex, named cytochrome *ba*, was isolated from the membranes of *A. ambivalens*. Two bands were observed in a SDS-PAGE with apparent molecular masses of 39 kDa and 51 kDa (Fig.

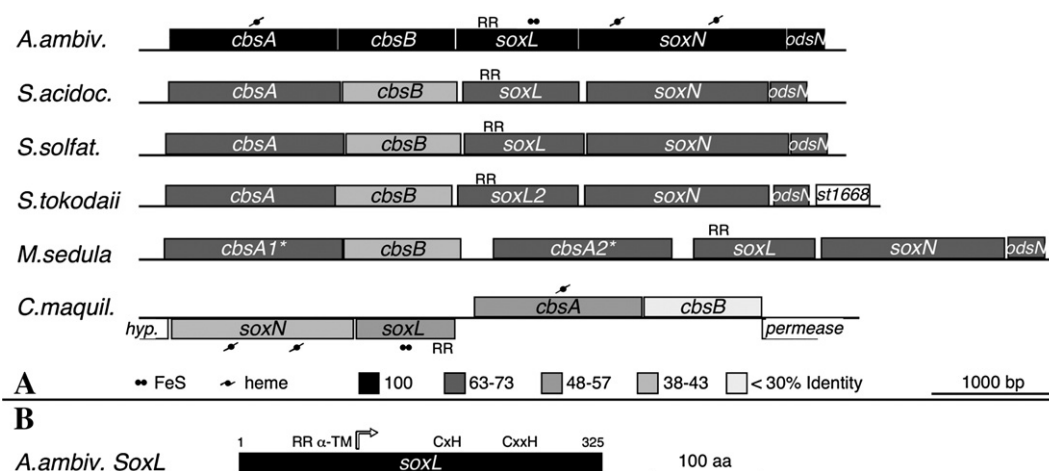


**Fig. 2.** (A) Comparison of the physical organization of the *A. ambivalens* *cbsAB-soxLN-odsN* locus with other members of the Sulfolobales. *S. tokodaii* *odsN* is not annotated in the genome sequence. The shading represents percentage range of amino acid sequence identities compared to the *A. ambivalens* proteins. Accession numbers: *A. ambivalens*, this work (AJ889917); *S. acidocaldarius*, NC\_007181; *S. solfataricus*, NC\_002754; *S. tokodaii*, NC\_003106; *Metallospaera sedula*, NC\_009440; *Caldivirga maquilingsensis*, NZ\_AAXQ00000000. (B) Domain organization of the *A. ambivalens* SoxL protein.

1). The latter subunit also stained with Alcian Blue suggesting a significant degree of glycosylation (Fig. 1).

### 3.1. The *cbsA* and *soxN* genes are part of a larger operon

The N-terminal amino acid sequences of the subunits of the cytochrome *ba* complex are SFPTIVAYKVVGLANLLGP and SYSKRISNAFNERLKLDDLP for the 39 kDa and the 51 kDa subunits, respectively (Supplementary Figs. S1 and S4). These N-termini identified the subunits as the products of the *cbsA* (cytochrome *b* from *Sulfolobus* [26]) and *soxN* (*Sulfolobus* oxidase [27]) genes, respectively.

The genes *cbsA* and *soxN* are part of a gene locus containing three other genes, organized as *cbsAB–soxLN–odsN* (Fig. 2). Comparison of the structural organization and sequences of the encoded proteins with the ones from other Crenarchaeota showed a high degree of similarity among them (Fig. 2 and Supplementary Figs. S1–S5) [15,26]. The *cbsA*

gene is followed by *cbsB*, encoding a hydrophobic transmembrane protein. In the Sulfolobales, it is followed by *soxL*, encoding a Rieske protein, *soxN* and *odsN*. The CbsB, SoxL, and OdsN proteins were not identified in *A. ambivalens* so far. The *odsN* gene (open reading frame downstream *soxN* [15]) encodes a small soluble protein of unknown function as proposed previously from the *S. acidocaldarius* and *S. solfataricus* genome sequences; however, it had not been annotated in the *S. tokodaii* genome [15]. In this genome, we found the homolog in a gap in between ST1667 (*soxN*) and ST1668 (hypothetical protein) when allowing alternative start codons (TTG; Fig. 3). Thus the entire *cbsAB–soxLN–odsN* gene cluster is present in the three *Sulfolobus* genomes and in *A. ambivalens*, while in *Metallosphaera sedula* the gene order is different and comprises an additional paralog of *cbsA* (Fig. 2) [28]. Interestingly, the anaerobic or microaerobic sulfate reducer archaeon *Caldivirga maquilingensis* also contains a *cbsAB–soxLN* cluster, but with a different gene organization and lacking the *odsN* gene (Fig. 2).

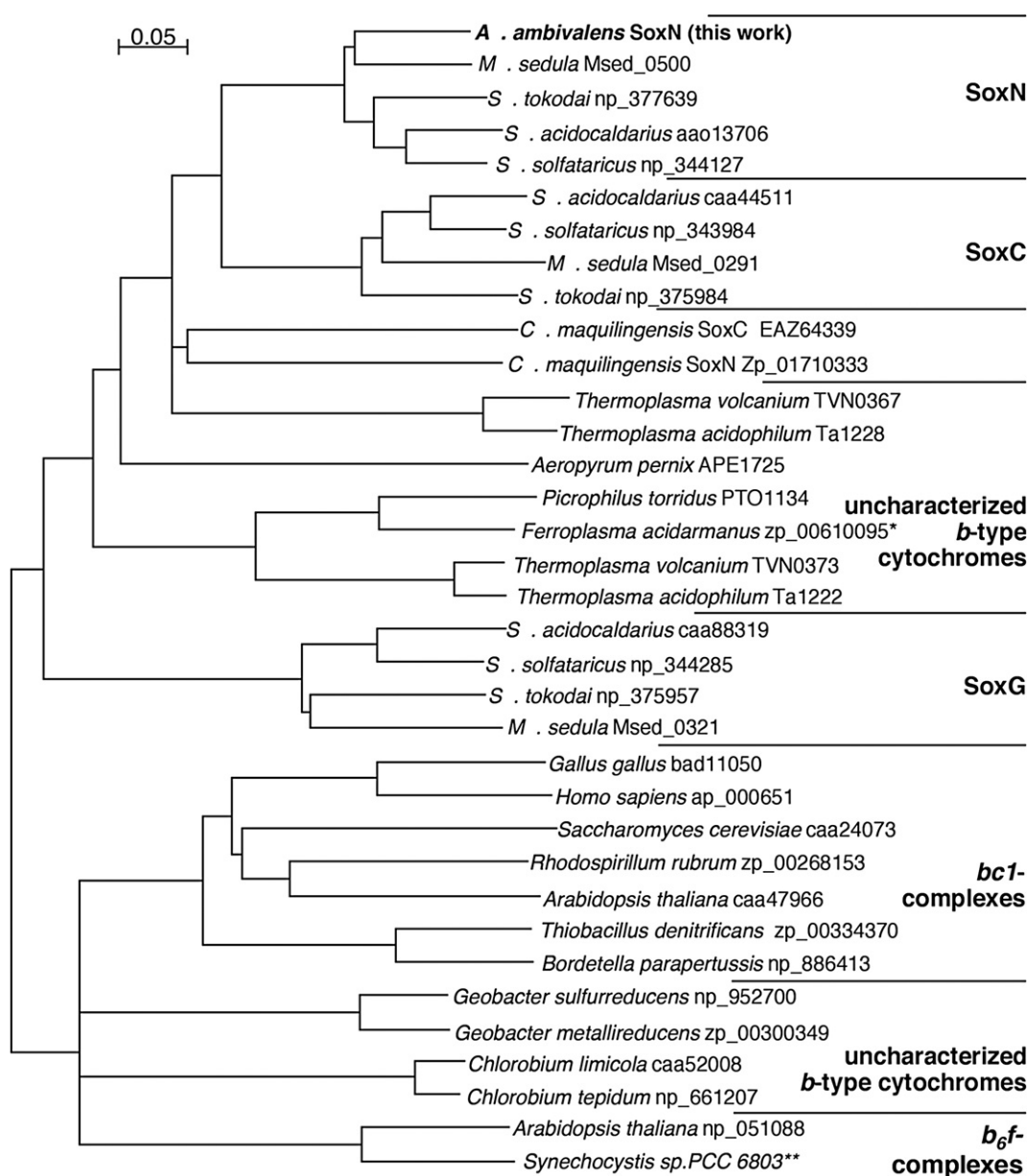


**Fig. 3.** Dendrogram of the archaeal SoxN, SoxC and SoxG amino acid sequences, with the cytochrome *b* subunits of bacterial and eukaryal *bc*<sub>1</sub> and *b*<sub>6</sub>*f* complexes. Dendrogram is based on the 260 most conserved amino acid positions of the multiple alignment (Supplementary Fig. S4). \*The database entry of the *Ferroplasma* cytochrome *b* amino acid sequence was incomplete. \*\*The *Synechocystis* cytochrome *b* sequence was concatenated from two proteins encoded as separate ORFs: PetB (baa10149) and PetD p27589. Accession or ORF numbers are indicated in front of the organism name.

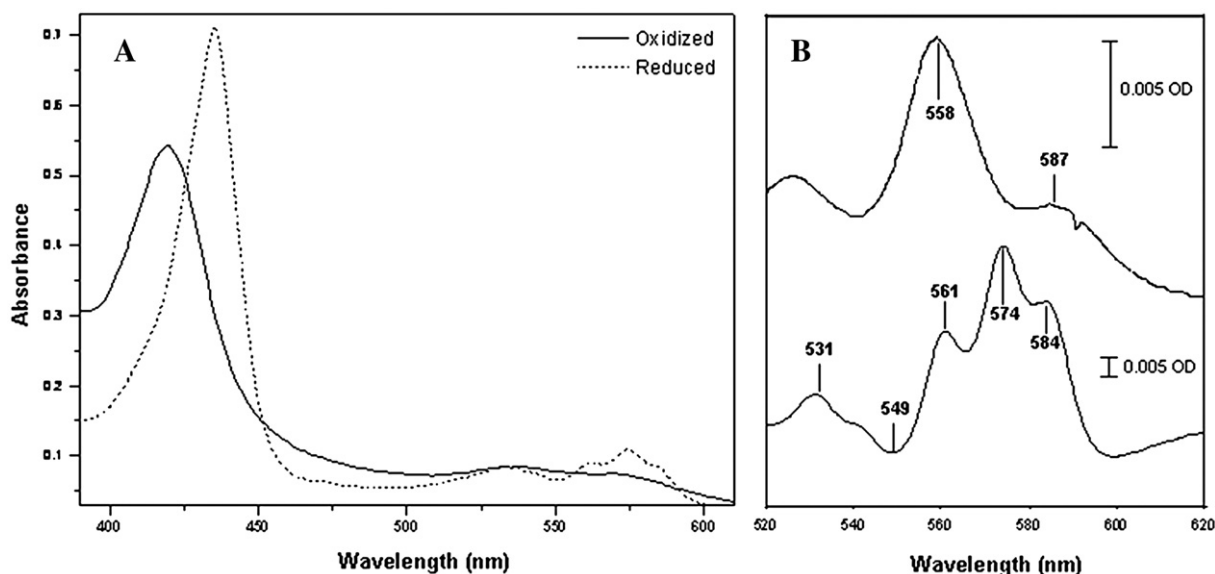


**Fig. 4.** UV-visible spectra of the *A. ambivalens* cytochrome *ba* complex. Panel A—UV-visible spectra of the oxidized and reduced complex ( $\sim 3.3 \mu\text{M}$ ); Panel B—Upper spectrum—pyridine hemeochrome difference spectrum of the enzymatic complex; lower spectrum difference of the spectra in panel A (sodium dithionite-reduced cytochrome *ba* complex minus potassium hexachloroiridate-oxidized enzyme).

### 3.2. *CbsA* is an analog of cytochrome *c*<sub>1</sub> and *SoxN* belongs to the *b*-type cytochrome superfamily

The sequence predicted from the *cbsA* ORF includes 29 amino acid residues, which were absent in the mature protein. These residues showed the typical composition of a signal peptide consisting of 3 basic amino acid residues followed by a hydrophobic stretch that could eventually form a transmembrane helix (Supplementary Fig. S1). Topology prediction revealed another putative transmembrane  $\alpha$ -helix in the C-terminus. Similarly to the cytochrome *c*<sub>1</sub> subunit of the bovine *bc*<sub>1</sub> complex [29], the C-terminal helix of *CbsA* may anchor the protein to the membrane while the remaining hydrophilic protein core extends into the periplasm. Building of a structural model was hampered due to the lack of similarity to any known protein. Two histidine and two methionine residues (H78, H186, M219 and M316), which may be the heme ligands, are well conserved among the homologous sequences from the closely related Sulfolobales (Supplementary Fig. S1). The mature *CbsA* of *A. ambivalens* is a 421 amino acid residue protein with a calculated molecular mass of 46 kDa, which is slightly higher than the one observed in SDS-PAGE (Fig. 1). The *A. ambivalens* *CbsA* subunit was not stained with Alcian Blue suggesting absence of glycosylation. This result is in contrast to the *S. acidocaldarius* *CbsA*, which was purified as a single-subunit protein containing several N-linked oligosaccharides and one O-linked mannose residue [26]. The lack of glycosylation of the *A. ambivalens* *CbsA* can be partially explained by the absence of a serine/threonine-rich stretch present in the proteins of the other Sulfolobales near the C-terminus, typical for O-glycosylation (Supplementary Fig. S1). The *CbsA* protein sequence is 60–80% identical to those present in the Sulfolobales group and 49% to that of *C. maquilingensis*. Interestingly, there is a second paralog in the facultative chemolithotrophs *S. tokodaii*, *M. sedula* and *S. metallicus* with about 30–35% amino acid identity. The *S. metallicus* *foxC* is similar to *cbsA* and is part of a larger operon encoding an oxygen reductase complex whose transcription was specifically induced when the organism was grown on iron instead of sulfur [30].

*SoxN* is a 553 amino acid residues protein with a calculated molecular mass of 62 kDa (Supplementary Fig. S4). The protein has a lower apparent molecular mass in SDS-PAGE despite the glycosylation (Fig. 1). However, this effect is frequently observed in transmembrane proteins. Topology prediction shows a profile of 12 transmembrane  $\alpha$ -helices. The typical heme-coordinating histidine residues from *b*-type

cytochromes of *bc*<sub>1</sub> and *b<sub>6</sub>f* complexes are present in conserved positions and relative distances, supporting the hypothesis that the *A. ambivalens* *ba* complex is a *bc*<sub>1</sub>-analogous complex (Supplementary Fig. S4). Furthermore, the *SoxN* 3D structural model (data not shown) predicts that the hemes are placed close to opposite sides of the membrane taking into account the location of the histidyls. These histidine residues are also predicted to have their lateral chain turned towards the inside where the hemes are likely to bind. Observation of this model and amino acid sequence comparisons allowed locating the quinol oxidation site (*Q<sub>o</sub>*) with the relevant conserved residues (e.g., M125, F129, Y132, P271, F275 and Y279) of the chicken *bc*<sub>1</sub>-complex within *A. ambivalens* *SoxN* (M127, F131, Y134, P290, F294 and Y298) [31]. The conserved residue of the quinone reduction site (*Q<sub>i</sub>*) (e.g., F221 in chicken and M221 in yeast *bc*<sub>1</sub>-complexes [31,32]) is also present in *SoxN* (F227). The chicken and bovine cyt *b* *Q<sub>o</sub>* site, comprising the highly conserved motif P<sub>271</sub>EWYF<sub>275</sub>, and the highly similar yeast homologue, P<sub>271</sub>EWYL<sub>275</sub>, can be compared with the motif detected in the *A. ambivalens* analogue complex, P<sub>290</sub>PWFF<sub>294</sub>, where the glutamate residue (E272) is replaced

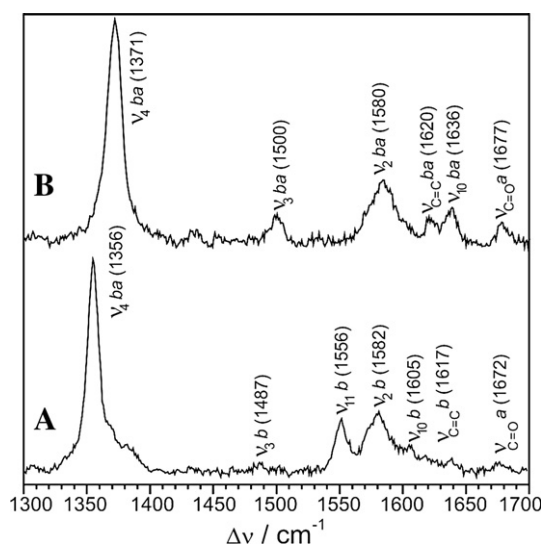


**Fig. 5.** Resonance Raman spectra of cytochrome *ba* complex in (A) fully reduced and (B) fully oxidized forms, measured with 413 nm excitation.

by a proline residue (P291) and the tyrosyl (Y274) is replaced by a phenylalanine residue (F294).

Regarding the  $Q_i$  site conserved residues; the *A. ambivalens ba* complex is less similar to the canonical cyt *b* complexes. Only the phenylalanine residue (F227) is conserved in the same position of the conserved F221. The amino acid residues  $K_{228}D_{229}$  are not present in the *A. ambivalens* complex, neither the histidyl (H202). The presence of the second quinone binding site supports the hypothesis that a  $Q$ -cycle mechanism is operative in the *A. ambivalens* complex III analogue.

It was found previously that SoxN was similar not only to the cytochrome *b* subunits of the bacterial and eukaryal  $bc_1$  and  $b_6f$  complexes but also to the paralogous SoxC (cytochrome *b* subunit from the quinol oxidase SoxABC [27]) and SoxG subunits of other respiratory complexes in the three *Sulfolobus* species, whose genomes were sequenced [15]. In fact, many of the genes coding for this protein are misannotated because they all share some mutual similarity. Here, we show based on a dendrogram calculation and using more archaeal sequences available, that the three paralogous SoxN, SoxG and SoxC proteins from the Sulfolobales form distinct clades (Fig. 3 and Supplementary Fig. S4). They are separated from each other at least as deeply as the subunits of the bacterial  $bc_1$  and  $b_6f$  complexes, which may point to gene duplication events very early in archaeal evolution. Even more striking is the deep bifurcation between archaeal and the combined bacterial and eukaryal *b* type cytochromes. This observation may indicate an early appearance of these proteins in the "last universal common ancestor" (LUCA) prior to the split into the three life domains or to a later lateral gene transfer. It should be noted that the dendrogram does not reflect the relationship of the different organisms but rather testifies of repeated gene duplication events

after separation into the three domains followed by speciation for use in different complexes.

### 3.3. Spectroscopic characterization of the cytochrome *ba* complex

The *A. ambivalens* purified *ba* complex is isolated in different partially reduced forms, most probably due to the high reduction potential of the hemes (see below). In the oxidized state, the cytochrome *ba* complex from *A. ambivalens* shows maxima in the Soret region at 419 nm, and at 570 and 535 nm in the  $\alpha$  and  $\beta$  regions, respectively. The difference of the spectra of the reduced and the oxidized protein exhibits maxima at 561, 574 and 584 nm in the  $\alpha$  band region, and a maximum at 531 in the  $\beta$  band region (Fig. 4A). The complex is reduced by ubiquinol even aerobically and the reduced form thus obtained is stable over time.

The pyridine hemeochrome spectrum (Fig. 4B) has maxima at 558 nm and 587 nm, indicating the presence of *b* and *a*-type hemes in the protein complex in a 2:1 ratio, respectively. HPLC analysis confirmed the heme stoichiometry and clearly identified heme *a* as an  $a_s$ -type heme by comparison with the heme extracted from *A. ambivalens aa\_3* oxygen reductase, which also contains  $a_s$  hemes. A stoichiometry of 3:1 of iron:protein was obtained by metal analysis. Interestingly, for the homologous *Sulfolobus acidocaldarius* complex [15,26] it was postulated that only *b*-type hemes were present in the heme-containing subunits. However, this conclusion was largely derived from analogy to the paralogous SoxC protein, which is part of the SoxM supercomplex, and to  $bc_1$  complexes, whereas SoxN was never purified from *S. acidocaldarius*.

The spin states of the heme groups can be determined from the Resonance Raman (RR) spectra of the *ba* complex, (Fig. 5). The most

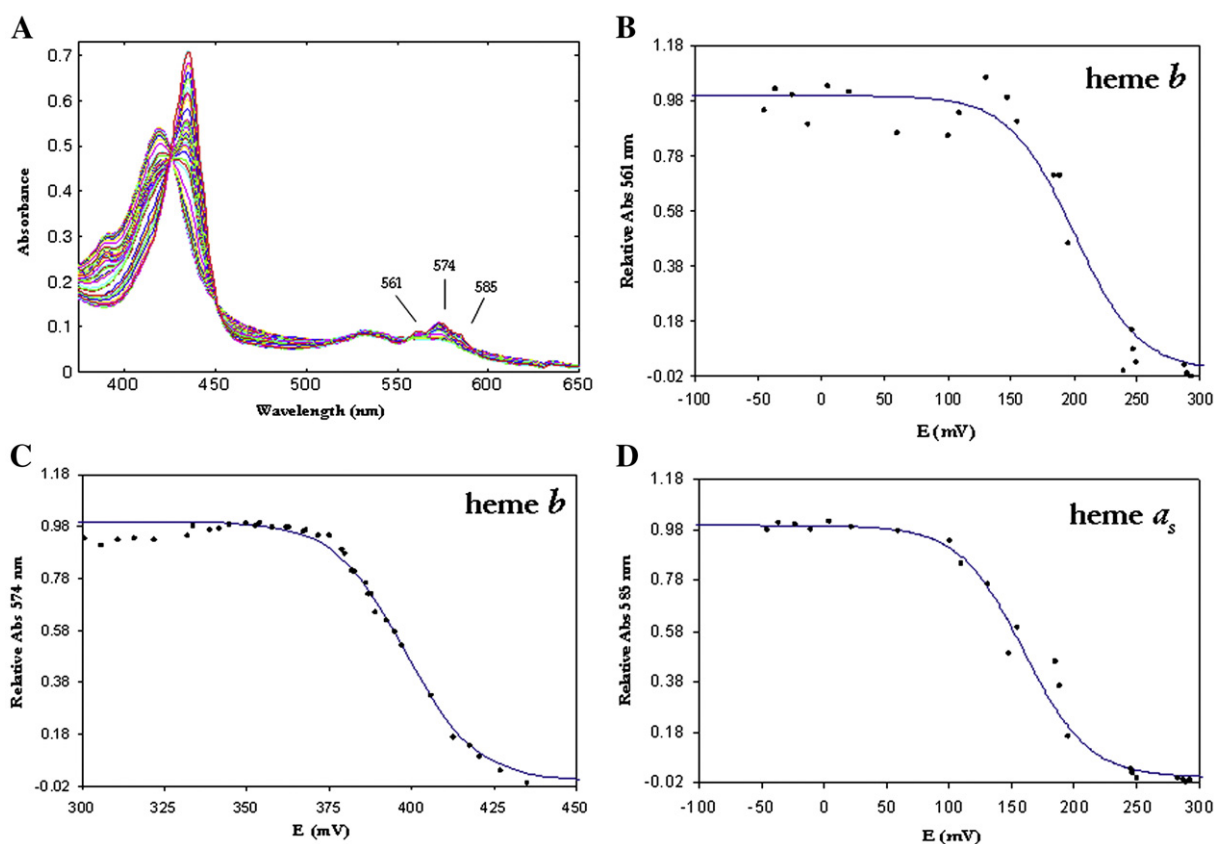


Fig. 6. Redox titration of the *A. ambivalens ba* complex. Panel A— UV-visible spectra of the cytochrome *ba* complex ( $\sim 3.3 \mu\text{M}$ ) along the redox titration. Panels B–D— absorption changes at 561, 574 and 585 nm, respectively, as a function of redox potential, at pH 6.5. The solid lines correspond to Nernst equations for one electron, with  $E = +200$ ,  $+400$  and  $+160$  mV, respectively.

prominent band,  $\nu_4$ , of cytochrome *ba* appears at 1356 and 1371  $\text{cm}^{-1}$  in the reduced (Fig. 5A) and oxidized (Fig. 5B) forms, respectively. Although the  $\nu_4$  peak position does not allow for a distinction between the different hemes it constitutes a reliable marker for the oxidation state. The Lorentzian shapes and band widths indicate that the spectra correspond to the fully reduced and fully oxidized protein, respectively. The broad line width of the  $\nu_4$  mode of the oxidized protein points to a presence of more than one heme group.

The RR spectrum of the *ba* complex in the reduced form (Fig. 5A) is largely dominated by the spectral contribution of hemes  $b^{2+}$ . The pre-emergence of the  $b^{2+}$  contribution is partially due to the fact that, according to the HPLC data (see above), the complex possesses 2 hemes *b* and only one heme *a*. In addition, the resonance enhancement for  $b^{2+}$  is expected to be stronger due to the larger absorbance at 413 nm compared to  $a^{2+}$ . This is particularly evident in the 1500–1700  $\text{cm}^{-1}$  region. First, the strong band at 1556  $\text{cm}^{-1}$  is a characteristic feature of *b*-type six-coordinated low-spin hemes that is assigned to the  $\nu_{11}$  mode. For six-coordinated low-spin  $a^{2+}$  hemes this mode shifts down to ca. 1520  $\text{cm}^{-1}$  [33,34].

The broad feature at 1582  $\text{cm}^{-1}$  is mainly due to the  $\nu_2$  mode of the six-coordinated low-spin hemes  $b^{2+}$ . The corresponding mode of the six-coordinated low-spin heme  $a^{2+}$  is expected at approximately the same position but its contribution to the 1582- $\text{cm}^{-1}$  band is likely to be low in view of the poorer resonance enhancement and lower relative content with respect to heme *b*. The position of the weak band at ca. 1487  $\text{cm}^{-1}$  is in good agreement with the  $\nu_3$  mode of a six-coordinated low-spin heme and, therefore, is attributed to  $b^{2+}$ . Thus, the RR spectrum of the fully reduced cytochrome *ba* complex provides strong evidence that both hemes *b* are in the six-coordinated low-spin configuration, but no clear information about heme *a*. However, this is due to the fact that, similarly to *ba*<sub>3</sub> oxygen reductase from *Thermus thermophilus*, the RR spectra of the *ba* complex are largely dominated by the bands of six-coordinated low-spin  $b^{2+}$ . As in the case of the *ba*<sub>3</sub> oxidase [33], the only band that can be unambiguously attributed to heme *a* is the weak feature at 1672  $\text{cm}^{-1}$  that is assigned to the formyl stretching [33].

Due to the fact that the oxidized hemes  $b^{3+}$  and  $a^{3+}$  exhibit a comparably strong absorbance at 413 nm, the RR spectrum of the fully oxidized protein excited at this wavelength (Fig. 5B) should display relatively stronger contributions of heme  $a^{3+}$ . In fact, the relative intensity of the formyl stretching of  $a^{3+}$  at 1677  $\text{cm}^{-1}$  has increased. Asymmetric bands at 1580, 1620 and 1636  $\text{cm}^{-1}$  include contribution of both types of hemes and are assigned to  $\nu_2$ ,  $\nu_{c=c}$  and  $\nu_{10}$  modes respectively. Their positions are characteristic of six-coordinated low-

spin ferric hemes. Specifically, we note a distinct band at 1500  $\text{cm}^{-1}$ , assigned to the  $\nu_3$  of a ferric six-coordinated low-spin heme, which exhibits an asymmetric line shape suggesting more than one component with similar frequencies. However, no band can be detected at frequencies between 1490 and 1475  $\text{cm}^{-1}$  that would indicate the existence of a ferric high-spin species. Thus, RR spectroscopy shows that all heme groups of the *ba* complex are in a six-coordinated low-spin configuration in the oxidized and most likely also in the reduced state. This finding represents yet another analogy between the *ba* and the *bc*<sub>1</sub> complexes. Particularly remarkable is the high frequency of the formyl stretching in both redox states which indicates only weak hydrogen bond interactions with the protein environment [33,34].

### 3.4. Redox titrations of the cytochrome *ba* complex

The reduction potentials of the cytochrome *ba* hemes were determined by redox titrations at pH 6.5, monitored by visible absorption spectroscopy. The spectra were recorded after the stepwise anaerobic addition of sodium dithionite (Fig. 6, Panel A). The Soret region of the spectrum changes upon reduction, from a maximum at 419 nm in the fully oxidized state to a maximum at 435 nm in the fully reduced state, with an isosbestic point at 426 nm. In the  $\alpha$ -band region three predominant bands at 561, 574 and 585 nm are observed upon reduction, corresponding to two *b* and one *a*<sub>s</sub> type heme, respectively. The changes in the absorption intensities at 561, 574 and 585 nm were plotted against the solution redox potential (Fig. 6, Panels B, C and D). The assignment of each band to a particular heme allowed for the determination of the respective reduction potentials. The *b* type hemes with absorption maxima at 561 and 574 nm show reduction potentials of +200 and +400 mV, respectively. The *a*<sub>s</sub> type heme (maximum at 585 nm) has a reduction potential of +160 mV.

According to the mechanism of the canonical *bc*<sub>1</sub>-complex (Q-cycle), the *b*-type cytochrome (SoxN protein in the *A. ambivalens* complex) may catalyze the electron transfer to the high potential cytochrome *c*<sub>1</sub> (CbsA protein in *A. ambivalens* complex) via the Rieske protein. Therefore, it is proposed that the highest reduction potential heme (*b* type heme,  $E = +398$  mV) is present in the CbsA protein, which is further supported by analogy with the *S. acidocaldarius* CbsA homologue also containing a *b*-type heme with a reduction potential of +400 mV [26]. According to this assignment, the di-hemic SoxN protein thus contains one *a*<sub>s</sub> and one *b* type heme, with reduction potentials of +160 and +200 mV, respectively.

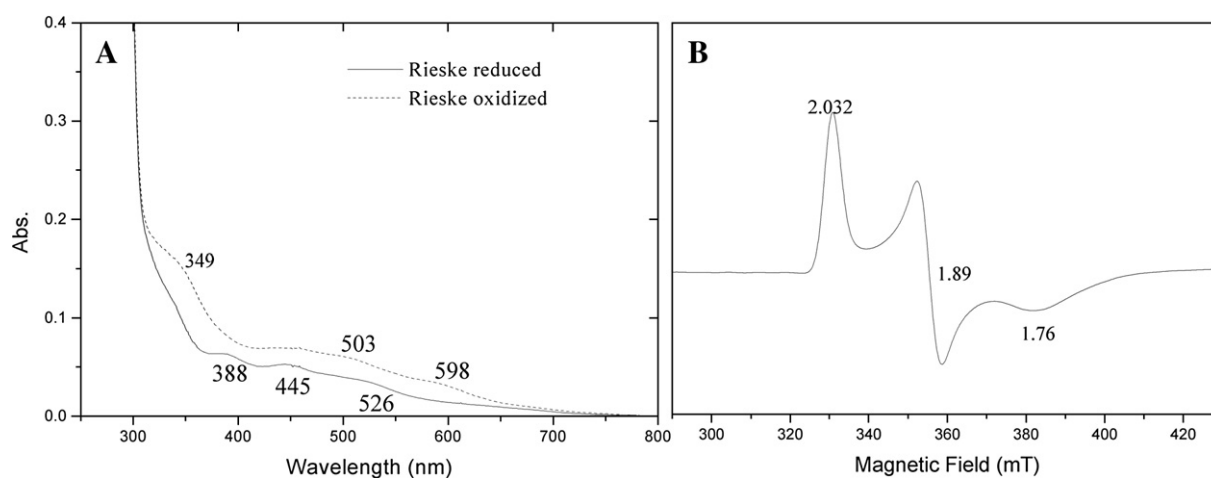


**Fig. 7.** Spectroscopic characterization of the heterologously expressed Rieske protein, the product of the *SoxL* gene. Panel A—UV-visible spectra of the protein in the oxidized and reduced state. Panel B—EPR spectrum of the Rieske protein in the reduced state. Experimental EPR conditions: microwave frequency, 9.39 GHz; microwave power: 2.0 mW, modulation amplitude: 1 mT, temperature 10 K. Principal  $g$ -values  $g_{\text{max}} = 2.032$ ;  $g_{\text{med}} = 1.89$  and  $g_{\text{min}} = 1.76$ .



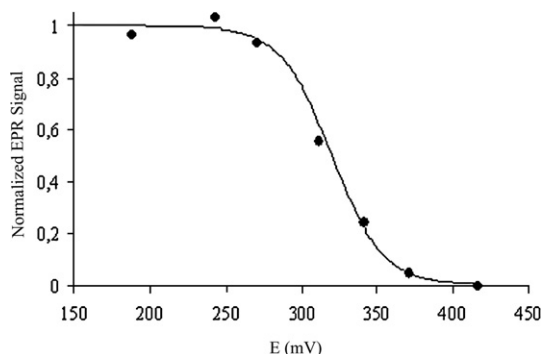


**Fig. 8.** Redox titration of the *A. ambivalens* Rieske protein monitored by EPR spectroscopy. Experimental conditions as in Fig. 7. The changes in EPR intensity were monitored at  $g=1.89$ . The solid line corresponds to a Nernst equation for one electron with  $E^{\circ}=+320$  mV.

### 3.5. SoxL, the Rieske protein

The *soxL* gene encodes a Rieske protein, which contains the strictly conserved motifs for the  $[2\text{Fe-2S}]^{2+/1+}$  cluster (CxHLGC and CPCHGSxY; Supplementary Fig. S3). SoxL has not yet been detected in *A. ambivalens*. However, the *soxL* gene transcription in vivo was demonstrated by the observation of a 800 bp PCR product obtained by reverse transcriptase PCR (data not shown).

The putative 325 amino acid residue translation product differs significantly from other Rieske proteins from  $bc_1$  and  $b_6f$  complexes in two aspects: (1) the amino acid sequence contains a twin arginine protein translocation signal sequence approximately 60 amino acid residues downstream of the start codon, and it is immediately followed by a predicted transmembrane  $\alpha$ -helix. The same is true for the homologous SoxL2 and SoxF proteins from *Sulfolobus* spp (Fig. 2B). It is not clear whether the mature *A. ambivalens* protein contains this unusually long 80 amino acid residue signal sequence. The distance between the two conserved iron-sulfur binding motifs is 50–60 amino acid residues compared to approximate 20 amino acid residues present in canonical Rieske proteins.

The *soxL* gene was expressed in *E. coli* in two versions, with and without the signal sequence. Only the short version produced a red protein with typical Rieske type UV-visible spectra in the reduced and oxidized forms, and an EPR spectrum of the reduced form with  $g$  values of 2.032, 1.89 and 1.76 (Fig. 7). The reduction potential of the Rieske protein, determined by a redox titration monitored by EPR spectroscopy, was +320 mV, at pH 7.4 (Fig. 8).

Three different Rieske proteins are found in most of the Sulfolobales genomes, SoxL, SoxL2 and SoxF. The first two are mutually similar (50–80% identity) but their genes are located in different clusters. SoxL is part of the *cbsAB-soxLN-odsN* operons, whereas the *soxL2* is usually found in conjunction with the *soxABC* quinol:oxygen oxidoreductase genes.

### 3.6. CbsB and OdsN

The *cbsB* gene encodes a putative hydrophobic protein with 311 amino acid residue protein and with a calculated molecular mass of 35 kDa, with 9 predicted transmembrane  $\alpha$  helices and has no obvious motifs for cofactor binding. This protein was not present in any of the *A. ambivalens* cytochrome *ba* complex preparations. Similarly, the gene is present in the other Sulfolobales but the protein has never been observed [15,26]. Homologs of *cbsB* (like in the case of *cbsA*) were only identified in the *Sulfolobus* spp., *Metallosphaera*, and *Caldivirga* genomes (Fig. 2, Supplementary Fig. S2).

The *odsN* gene present in the same locus encodes a soluble 12 kDa protein, containing no obvious motifs for binding of prosthetic

groups. It has 62% identity with its homologue from *Sulfolobus acidocaldarius*, which is annotated as an RNAase in Genbank (Accession No. AAO13707 [15]). A closer inspection of BLAST results and alignments revealed that the protein is conserved not only in the Sulfolobales but also in numerous other Archaea and also in some Bacteria (Fig. 2; see Supplementary Fig. S5). This protein was isolated neither from *Sulfolobus* nor *Acidianus* cells.

### 3.7. The *A. ambivalens* cytochrome *ba* complex is analogous to $bc_1$ complex

In summary here we described a novel type of cytochrome isolated from the membranes of aerobically grown cells of the thermoacidophilic archaeon *A. ambivalens*.

This complex is analogous to the  $bc_1$  complex present in bacteria and eukarya, which was so far unknown in Archaea. The gene cluster coding for that new complex is composed of five different genes *cbsAB-soxLN-odsN*. The  $a_s$  isolated protein consists of two subunits encoded by the genes *cbsA* and *soxN*. The latter has significant structural homology with the *b*-type cytochromes of  $bc_1$ -complexes, while the protein encoded by *soxL*, expressed in *E. coli*, shows clear similarities with the Rieske proteins of these complexes. The presence of CbsA and CbsB was specifically predicted in the Sulfolobales, with CbsA likely replacing the cytochrome  $c_1$ . Thus, we suggest that the electron flow in this novel  $bc_1$ -analogous complex is similar to the one observed in Bacteria or Eukarya and likewise can be operative through a Q-cycle mechanism.

### Acknowledgments

M. Regalla (ITQB) is acknowledged for protein N-terminal sequencing and HPLC heme determination. P.N.R. is recipient of a grant from Fundação para a Ciência e a Tecnologia (BD SFRH XXI/BD/24745/2005). This work was supported by Fundação para a Ciência e a Tecnologia (POCI/QUI/59824/2004 to MMP and POCI/BIA-PRO/58608/2004 to MT) and by DFG (SFB498). Filipa L. Sousa is acknowledged for the glycosylation assays.

### Appendix A. Supplementary data

Supplementary data associated with this article can be found, in the online version, at [doi:10.1016/j.bbabi.2008.09.009](https://doi.org/10.1016/j.bbabi.2008.09.009).

### References

- [1] S. Anemuller, C.L. Schmidt, I. Pacheco, G. Schäfer, M. Teixeira, A cytochrome  $aa_3$ -type quinol oxidase from *Desulfurolobus ambivalens*, the most acidophilic archaeon, FEMS Microbiol. Lett. 117 (1994) 275–280.
- [2] T.M. Bandejas, M.M. Pereira, M. Teixeira, P. Moenne-Loccoz, N.J. Blackburn, Structure and coordination of CuB in the *Acidianus ambivalens*  $aa_3$  quinol oxidase heme-copper center, J. Biol. Inorg. Chem. 10 (2005) 625–635.
- [3] T.K. Das, C.M. Gomes, T.M. Bandejas, M.M. Pereira, M. Teixeira, D.L. Rousseau, Active site structure of the  $aa_3$  quinol oxidase of *Acidianus ambivalens*, Biochim. Biophys. Acta 1655 (2004) 306–320.
- [4] A. Giuffrè, C.M. Gomes, G. Antonini, E. D'Itri, M. Teixeira, M. Brunori, Functional properties of the quinol oxidase from *Acidianus ambivalens* and the possible catalytic role of its electron donor—studies on the membrane-integrated and purified enzyme, Eur. J. Biochem. 250 (1997) 383–388.
- [5] S. Todorovic, M.M. Pereira, T.M. Bandejas, M. Teixeira, P. Hildebrandt, D.H. Murgida, Midpoint potentials of hemes  $a$  and  $a_3$  in the quinol oxidase from *Acidianus ambivalens* are inverted, J. Am. Chem. Soc. 127 (2005) 13561–13566.
- [6] P. Mitchell, The protonmotive Q cycle: a general formulation, FEBS Lett. 59 (1975) 137–139.
- [7] X.H. Yang, B.L. Trumpower, Purification of a three-subunit ubiquinol-cytochrome  $c$  oxidoreductase complex from *Paracoccus denitrificans*, J. Biol. Chem. 261 (1986) 12282–12289.
- [8] P.O. Ljungdahl, J.D. Pennoyer, D.E. Robertson, B.L. Trumpower, Purification of highly active cytochrome  $bc_1$  complexes from phylogenetically diverse species by a single chromatographic procedure, Biochim. Biophys. Acta 891 (1987) 227–241.
- [9] A. Kriauciunas, L. Yu, C.A. Yu, R.M. Wynn, D.B. Knaff, The *Rhodospirillum rubrum* cytochrome  $bc_1$  complex: peptide composition, prosthetic group content and quinone binding, Biochim. Biophys. Acta 976 (1989) 70–76.

- [10] C.L. Schmidt, S. Anemuller, G. Schafer, Two different respiratory Rieske proteins are expressed in the extreme thermoacidophilic crenarchaeon *Sulfolobus acidocaldarius*: cloning and sequencing of their genes, *FEBS Lett.* 388 (1996) 43–46.
- [11] R. Ishikawa, Y. Ishido, A. Tachikawa, H. Kawasaki, H. Matsuzawa, T. Wakagi, *Aeropyrum pernix* K1, a strictly aerobic and hyperthermophilic archaeon, has two terminal oxidases, cytochrome *ba*<sub>3</sub> and cytochrome *aa*<sub>3</sub>, *Arch. Microbiol.* 179 (2002) 42–49.
- [12] A. Ruepp, W. Graml, M.L. Santos-Martinez, K.K. Koretke, C. Volker, H.W. Mewes, D. Frishman, S. Stocker, A.N. Lupas, W. Baumeister, The genome sequence of the thermoacidophilic scavenger *Thermoplasma acidophilum*, *Nature* 407 (2000) 508–513.
- [13] K. Sreeramulu, C.L. Schmidt, G. Schafer, S. Anemuller, Studies of the electron transport chain of the euryarchaeon *Halobacterium salinarum*: indications for a type II NADH dehydrogenase and a complex III analog, *J. Bioenerg. Biomembranes* 30 (1998) 443–453.
- [14] M. Lubben, S. Arnaud, J. Castresana, A. Warne, S.P. Albracht, M. Saraste, A second terminal oxidase in *Sulfolobus acidocaldarius*, *Eur. J. Biochem.* 224 (1994) 151–159.
- [15] A. Hiller, T. Henninger, G. Schafer, C.L. Schmidt, New genes encoding subunits of a cytochrome *bc*<sub>1</sub>-analogous complex in the respiratory chain of the hyperthermoacidophilic crenarchaeon *Sulfolobus acidocaldarius*, *J. Bioenerg. Biomembranes* 35 (2003) 121–131.
- [16] M. Teixeira, R. Batista, A.P. Campos, C. Gomes, J. Mendes, I. Pacheco, S. Anemuller, W.R. Hagen, A seven-iron ferredoxin from the thermoacidophilic archaeon *Desulfurolobus ambivalens*, *Eur. J. Biochem.* 227 (1995) 322–327.
- [17] S.F. Altschul, W. Gish, W. Miller, E.W. Myers, D.J. Lipman, Basic local alignment search tool, *J. Mol. Biol.* 215 (1990) 403–410.
- [18] J.D. Thompson, D.G. Higgins, T.J. Gibson, CLUSTAL W: improving the sensitivity of progressive multiple sequence alignment through sequence weighting, position-specific gap penalties and weight matrix choice, *Nucleic Acids Res.* 22 (1994) 4673–4680.
- [19] K. Katoh, K. Kuma, H. Toh, T. Miyata, MAFFT version 5: improvement in accuracy of multiple sequence alignment, *Nucleic Acids Res.* 33 (2005) 511–518.
- [20] C. Lambert, N. Leonard, X. De Bolle, E. Depiereux, ESyPred3D: prediction of proteins 3D structures, *Bioinformatics* 18 (2002) 1250–1256.
- [21] C. Watters, A one-step biuret assay for protein in the presence of detergent, *Anal. Biochem.* 88 (1978) 695–698.
- [22] D.E. Garfin, One-dimensional gel electrophoresis, *Methods Enzymol.* 182 (1990) 425–441.
- [23] E.A. Berry, B.L. Trumpower, Simultaneous determination of hemes *a*, *b*, and *c* from pyridine hemochrome spectra, *Anal. Biochem.* 161 (1987) 1–15.
- [24] M. Lubben, K. Morand, Novel prenylated hemes as cofactors of cytochrome oxidases. Archaea have modified hemes A and O, *J. Biol. Chem.* 269 (1994) 21473–21479.
- [25] P. Edman, G. Begg, A protein sequenator, *Eur. J. Biochem.* 1 (1967) 80–91.
- [26] T. Hettmann, C.L. Schmidt, S. Anemuller, U. Zahringer, H. Moll, A. Petersen, G. Schafer, Cytochrome b558/566 from the archaeon *Sulfolobus acidocaldarius*. A novel highly glycosylated, membrane-bound b-type hemoprotein, *J. Biol. Chem.* 273 (1998) 12032–12040.
- [27] M. Lubben, B. Kolmerer, M. Saraste, An archaeobacterial terminal oxidase combines core structures of two mitochondrial respiratory complexes, *EMBO J.* 11 (1992) 805–812.
- [28] U. Kappler, L.L. Sly, A.G. McEwan, Respiratory gene clusters of *Metallosphaera sedula* – differential expression and transcriptional organization, *Microbiology* 151 (2005) 35–43.
- [29] S. Iwata, J.W. Lee, K. Okada, J.K. Lee, M. Iwata, B. Rasmussen, T.A. Link, S. Ramaswamy, B.K. Jap, Complete structure of the 11-subunit bovine mitochondrial cytochrome *bc*<sub>1</sub> complex, *Science* 281 (1998) 64–71.
- [30] S. Bathe, P.R. Norris, Ferrous iron- and sulfur-induced genes in *Sulfolobus metallicus*, *Appl. Environ. Microbiol.* 73 (2007) 2491–2497.
- [31] Z. Zhang, L. Huang, V.M. Shulmeister, Y.I. Chi, K.K. Kim, L.W. Hung, A.R. Crofts, E.A. Berry, S.H. Kim, Electron transfer by domain movement in cytochrome *bc*<sub>1</sub>, *Nature* 392 (1998) 677–684.
- [32] C. Hunte, J. Koepke, C. Lange, T. Rossmannith, H. Michel, Structure at 2.3 Å resolution of the cytochrome *bc*(1) complex from the yeast *Saccharomyces cerevisiae* co-crystallized with an antibody Fv fragment, *Structure* 8 (2000) 669–684.
- [33] S. Gerschler, P. Hildebrandt, G. Buse, T. Soulimane, The active site structure of *ba*<sub>3</sub> oxidase from *Thermus thermophilus* studied by resonance Raman spectroscopy, *Biospectroscopy* 5 (1999) S53–63.
- [34] G.E. Heibel, P. Hildebrandt, B. Ludwig, P. Steinrucke, T. Soulimane, G. Buse, Comparative resonance Raman study of cytochrome *c* oxidase from beef heart and *Paracoccus denitrificans*, *Biochemistry* 32 (1993) 10866–10877.